Hierarchical Composites Reinforced with Carbon Nanotube Grafted Fibers: The Potential Assessed at the Single Fiber Level

Hui Qian,[†,‡] Alexander Bismarck,[‡] Emile S. Greenhalgh,[§] Gerhard Kalinka,[△] and Milo S. P. Shaffer*,[†]

Department of Chemistry, Imperial College London, London SW7 2AZ, U.K.; The Polymer and Composite Engineering (PaCE) Group, Department of Chemical Engineering, Imperial College London, London SW7 2AZ, U.K.; The Composites Centre, Imperial College London, London SW7 2AZ, U.K.; and BAM-Federal Institute for Materials Research and Testing, Division V.6, D-12205 Berlin, Germany

Received September 27, 2007. Revised Manuscript Received December 3, 2007

The feasibility of reinforcing conventional carbon fiber composites by grafting carbon nanotubes (CNTs) onto the fiber surface has been investigated. Carbon nanotubes were grown on carbon fibers using the chemical vapor deposition (CVD) method. Iron was selected as the catalyst and predeposited using the incipient wetness technique before the growth reaction. The morphology of the products was characterized using scanning electron microscopy (SEM), which showed evidence of a uniform coating of CNTs on the fiber surface. Contact angle measurements on individual fibers, before and after the CNT growth, demonstrated a change in wettability that can be linked to a change of the polarity of the modified surface. Model composites based on CNT-grafted carbon fibers/epoxy were fabricated in order to examine apparent interfacial shear strength (IFSS). A dramatic improvement in IFSS over carbon fiber/epoxy composites was observed in the single fiber pull-out tests, but no significant change was shown in the push-out tests. The different IFSS results were provisionally attributed to a change of failure mechanism between the two types of tests, supported by fractographic analysis.

Introduction

Carbon nanotubes (CNTs) are excellent candidates for a new generation of high-strength, high-stiffness materials due to their low density, high aspect ratio, and intrinsically superior mechanical properties to conventional materials.[1,2] Although promising results have been obtained, obtaining absolute improvements over existing high-performance materials has proved challenging. Interest is, therefore, growing in the improvement of conventional high-performance composites using CNTs, in particular, the development of hierarchical composite materials based on CNT-grafted fibers.[3,4] The intention is that the presence of CNTs in the matrix may alleviate many of the drawbacks of conventional fiber composites, especially longitudinal compression and interlaminar properties. A small number of reports[5,6] have looked at CNTs randomly dispersed into thermosetting matrices prior to infiltration, but viscosity and self-filtration issues severely limit the concentration of CNTs that can be incorporated. Grafting the nanotubes onto the conventional fiber surface, on the other hand, has the potential to provide higher loadings of CNTs with a radial orientation that may be optimal for transverse reinforcement.

The fiber/matrix interface has been the subject of numerous studies over the past few decades. Efforts have been made to improve the interfacial adhesion using various methods,[7–11] by either enhancing the chemical activity of the fiber surface or increasing the surface area. The magnitude of improvement in the interfacial shear stress (IFSS) of carbon fiber/epoxy composites has been very variable, depending on the fiber and matrix combinations; increases in the range 17−217% have been reported when using thermal treatments[8] and electrochemical oxidations[9] to modify the carbon fibers. Grafting carbon fibers with CNTs is likely to improve the fiber−matrix interfacial strength, which will enhance the adhesion and thus improve the composite delamination resistance. Unlike conventional approaches to improving IFSS, the nanotube should offer additional benefits. For example, reinforcement radial to the carbon fibers, extending into the surrounding matrix, will inhibit fiber microbuckling, which is a critical composite failure mode under compressive loading.[12]

* Corresponding author. E-mail: m.shaffer@imperial.ac.uk.
† Department of Chemistry, Imperial College London.
‡ Department of Chemical Engineering, Imperial College London.
§ The Composites Centre, Imperial College London.
△ BAM-Federal Institute for Materials Research and Testing.

(1) Harris, P. *Int. Mater. Rev.* **2004**, *49*, 31–43.
(2) Coleman, J. N.; Khan, U.; Blau, W. J.; Gun'ko, Y. K. *Carbon* **2006**, *44*, 1624–1652.
(3) Thostenson, E. T.; Li, W. Z.; Wang, D. Z.; Ren, Z. F.; Chou, T. W. *J. Appl. Phys.* **2002**, *91*, 6034–6037.
(4) Veedu, V. P.; Cao, A.; Li, X.; Ma, K.; Soldano, C.; Kar, S.; Ajayan, P. M.; Ghasemi-Nejhad, M. N. *Nat. Mater.* **2006**, *5*, 457–462.
(5) Fan, Z. H.; Hsiao, K. T.; Advani, S. G. *Carbon* **2004**, *42*, 871–876.
(6) Rutkofsky, M.; Ait-Haddou, H.; Folaron, R.; Criscuolo, L. "Zyvex Application Note 9715: Using Zyvex's NanoSolve Additive with Carbon Nanotubes for Enhanced Epoxy Composites", Zyvex.
(7) Wu, Z.; Pittman, J. C. U.; Gardner, S. D. *Carbon* **1995**, *33*, 597–605.
(8) Ramanathan, T.; Bismarck, A.; Schulz, E.; Subramanian, K. *Compos. Sci. Technol.* **2001**, *61*, 599–605.
(9) Deng, S. Q.; Ye, L.; Mai, Y. W. *Adv. Compos. Mater.* **1998**, *7*, 169–182.
(10) Rabotnov, J. N.; Perov, B. V.; Lutsau, V. G.; Ssorina, T. G.; Stepanitshev, E. I. *Carbon Fibers—Their Place in Modern Technology*; The Plastics Institute: London, 1974; pp 65–70.
(11) Downs, W. B.; Baker, R. T. K. *J. Mater. Res.* **1995**, *10*, 625–633.

10.1021/cm702782j CCC: $40.75
Published on Web 02/09/2008

Early work has been focused on growing carbon nanotubes onto the fiber surface using different catalyst systems and synthesis methods,[3,13–15] and a variety of morphologies and distributions of nanotubes have been reported; the CVD route has been established as the most effective and practical route to synthesizing CNTs in this context. However, the surface properties of CNT-grafted carbon fibers have not yet been studied, and only a few studies[3,4,11] have explored the interfacial and mechanical properties of the hierarchical composites. Downs and Baker[11] reported that the surface area was dramatically increased by around 300 times after the growth of nanofibers, a much greater effect than typically obtained with conventional "roughening" treatments,[16] which offer increases of less than a factor of 10. Downs et al.[11] also investigated the interfacial properties of the composites with carbon nanofiber-grafted carbon fibers through single fiber fragmentation tests and demonstrated that it was possible, in the best case, to obtain an improvement of over 4.75 times in the interfacial shear strength. In similar tests, Thostenson et al.[3] found an improvement of interfacial load transfer, attributed to local stiffening of the polymer matrix near the interface. It was recently reported that the mechanical properties of epoxy composites were improved without compromising the in-plane properties by coating 2D SiC woven fabric reinforcements with CNTs.[4]

In the present study, the feasibility of reinforcing conventional thermoset composites with CNT-grafted carbon fibers has been further investigated. CNTs were grown onto the fiber surface using the CVD method. Contact angle measurements were performed to examine the surface properties of the grafted fibers which are relevant to subsequent resin infiltration. Model composites with CNT-grafted fibers were fabricated to examine the interfacial shear strength using single fiber pull-out and push-out tests. A difference in failure mode was related to the effects of the grafting process on the microstructure and mechanical properties of the primary fibers.

Experimental Section

Materials. Unsized C320.00A (CA) PAN-based carbon fibers (~7.5 μm in diameter, Sigri, SGL-Carbon, Meitingen, Germany) were used for this work. To improve the surface chemical reactivity, the carbon fibers (CAox) were modified using a wet chemical method,[7,16] including an acid oxidation (65% HNO_3, Fluka), for 5 h, followed by a base wash (0.05 M NaOH, Fluka) for 24 h.

Grafting Process. The iron catalyst was introduced onto the oxidized carbon fibers using a 150 mM ethanol solution of $Fe(NO_3)_3 \cdot 9H_2O$ (A.C.S. reagent, Aldrich) via the incipient wetness technique; a final iron loading of 0.4 wt % was achieved. The growth of CNTs on the catalyst predeposited fibers (NT-CAox) was achieved by using acetylene (C_2H_2) as the hydrocarbon source by the CVD method in a tubular quartz furnace (~50 mm in diameter). A 10% H_2/Ar mixture was used as the carrier gas. The reactions were performed at 750 °C for 1 h using a 1:200 flow ratio of C_2H_2 to carrier gas. To improve the surface activity of the CNT-grafted carbon fibers (Oxi NT-CAox), thermal oxidation was carried out in air at 300 °C for 1 h. The modified carbon fibers were characterized using a field emission gun scanning electron microscope (Gemini LEO 1525 FEG-SEM, Carl Zeiss NTS GmbH).

Contact Angle Measurements. Contact angle measurements were performed using the modified Wilhelmy technique.[17] The following test liquids were used; deionized water (H_2O) $\gamma_l = 72.8$ mN/m with a polar component γ_l^p of 50.7 mN/m and a dispersive component of the surface of the surface tension γ_l^d of 22.1 mN/m), diiodomethane (DIM) ($\gamma_l = 50.8$ mN/m with $\gamma_l^p = 6.7$ mN/m, $\gamma_l^d = 44.1$ mN/m, 99% purity, Fisher Scientific), and epoxy resin ($\gamma_l = 42.5$ mN/m, HexPly 8552, Hexcel Composites). The surface tension of the epoxy resin was measured on a K100 processor tensiometer (Krüss GmbH, Hamburg Germany) using the Wilhelmy plate method. In each measurement, five individual fibers were placed parallel to each other onto an aluminum carrier. Weight changes were recorded using an ultramicrobalance (4504 MP8, Sartorius, Germany; accuracy = 0.1 μg) during the fiber immersion−emersion cycle in the testing liquids at a speed of 4.2 μm/s. At least five measurements for each fiber sample were carried out. Advancing (θ_a) and receding (θ_r) contact angles were calculated from the weight changes, Δm, using Wilhelmy's equation:

$$\cos\theta = \frac{\Delta m g}{\pi d \gamma_l} \tag{1}$$

where g is the acceleration of gravity, d is the fiber diameter, and γ_l is the surface tension of the test liquid. The diameter of the fibers were measured using *n*-dodecane ($\gamma_l = 25.4$ mN/m, 99% purity, Fisher Scientific), which is able to wet the fibers completely ($\cos\theta = 1$) and possesses a relatively low evaporation rate.

The surface tensions of the investigated fibers were determined by the harmonic mean method introduced by Wu[18] which is valid for low-energy materials. On the basis of measured contact angles in a pair of test liquids with known γ_l, γ_l^p, and γ_l^d, the two surface tension components of the fibers, γ_s^p and γ_s^d, can be calculated (see details in ref 17), and the fiber surface tension, γ_s, is given by the equation

$$\gamma_s = \gamma_s^p + \gamma_s^d \tag{2}$$

while the polarity X^p is expressed as

$$X^p = \frac{\gamma_s^p}{\gamma_s} \tag{3}$$

In addition, the reversible thermodynamic work of adhesion, W_a, between the investigated fibers and the test liquids can be evaluated from the equation[19]

$$W_a = \gamma_l(1 + \cos\theta) \tag{4}$$

Single Fiber Tensile Tests. Single fiber tensile tests were carried out at room temperature, according to the British industrial standard ISO 11566:1996 using a TST 350 tensile stress testing system (Linkam Scientific Instrument Ltd.) equipped with a 20 N force sensor. A single fiber was glued at either end onto a small piece of cardboard for better handling. The gauge lengths were 15, 25, and

(12) Jelf, P. M.; Fleck, N. A. *J. Compos. Mater.* **1992**, *26*, 2706–2726.
(13) Zhu, S.; Su, C. H.; Lehoczky, S. L.; Muntele, I.; Ila, D. *Diamond Relat. Mater.* **2003**, *12*, 1825–1828.
(14) Zhao, Z. G.; Ci, L. J.; Cheng, H. M.; Bai, J. B. *Carbon* **2005**, *43*, 663–665.
(15) Cesano, F.; Bertarione, S.; Scarano, D.; Zecchina, A. *Chem. Mater.* **2005**, *17*, 5119–5123.
(16) Donnet, J. B.; Wang, T. K.; Peng, J. C. M.; Rebouillat, S. *Carbon Fibers*, 3rd ed.; Marcel Dekker: New York, 1998.
(17) Bismarck, A.; Kumru, M. E.; Springer, J. *J. Colloid Interface Sci.* **1999**, *210*, 60–72.
(18) Wu, S. *Polymer Interface and Adhesion*; Dekker: New York, 1982.
(19) Bismarck, A.; Richter, D.; Wuertz, C.; Springer, J. *Colloids Surf., A* **1999**, *159*, 341–350.

35 mm. A typical crosshead speed of 15 μm/s was applied for the tests. A minimum of 25 measurements were recorded for each fiber specimen at each gauge length. The system compliance C was not insignificant and was estimated to be 0.7 mm/N under the relevant experimental conditions. The apparent elastic modulus was therefore corrected using the following equation (BS ISO 11566:1996 Method B):

$$E = E^* \Big/ \left(1 - C\,\frac{E^* A}{L}\right) \tag{5}$$

where C is the system compliance, E^* is the apparent modulus, derived from the gradient of the stress–strain curve, A is the cross-sectional area of the fiber, and L is the gauge length.

Interfacial Characterization. In an attempt to study the interfacial properties of the composites with CNT-grafted carbon fibers, a variety of techniques were exploited, including single fiber pull-out test, push-out test, and fractographic characterization. An epoxy matrix material (HexPly 8552) supplied by Hexcel Composites was used as the matrix. All these fiber/matrix composite specimens were cured at 110 °C for 1 h and 180 °C for 2 h as recommended by the manufacturer (Hexcel Composites, Product Data HexPly 8552, 2003).

In the pull-out test, a single fiber with a few millimeters in length was partly embedded at one end in epoxy on an aluminum sample carrier using an in-house apparatus.[20] The fiber was orientated perpendicular to the carrier surface and fixed to a force transducer. A variation of the embedded lengths in a range of 10–200 μm was allowed for the test. After the embedding, the diameter of each fiber specimen was measured by the laser light diffraction technique.[21] The pull-out test was performed on a high stiffness frame with a piezo-motor that allowed the force to be measured to an accuracy of $\pm$1 mN (see ref 22 for details of the equipment). The fiber was loaded at a speed of 0.2 μm/s from the matrix while the force was recorded against the displacement using a computer. The apparent interfacial shear strength, τ_{app}, was calculated from the peak pull-out force, F_{max}, and the fiber embedded area ($\pi d_f l$) using the following equation:[23]

$$\tau_{app} = \frac{F_{max}}{\pi d_f l} \tag{6}$$

where d_f is the fiber diameter and l is the embedded length. At least six measurements for each sample were recorded.

The principle of the push-out test is to push an embedded fiber in its axial direction until the interface fails under the arising shear stress. Fibers were laid flat into a small rod mold; resin was introduced and cured. The composite rod was embedded into a plastic cylinder for better handling. The bottom of the cylinder was first polished using a combination of Struers RotoForce-4 and RotoPol-31 (Struers GmbH). A 300–500 μm composite slice was then cut from the finished side of the cylinder by a saw microtome (SP1600, Leica Microsystems Nussloch GmbH). The final polishing was carried out on the other side of the cylinder using an accurate (within $\pm$1.5 μm) grinding machine (400 CS, EXAKT Technologies, Inc.) until the desirable slice thickness (15–40 μm) was reached. The push-out test was performed using an in-house apparatus.[24] An indenter with 5 μm in diameter was fixed to the force sensor, which was mounted, together with a reflecting light microscope, on a traveling head. Once the fiber was selected using the optical microscope, the two-position sample stage was switched from the position under the microscope to the one under the indenter. During subsequent movement of the indenter in the fiber direction, the applied force against the displacement was recorded. The apparent interfacial shear strength, τ_{app}, can be obtained using eq 6 where l is the specimen thickness, in this case. At least 10 fibers were pushed out from each sample.

For the fractographic analysis, fibers were laid flat into a small mold; resin was introduced and cured. The specimens were then fractured in bending, transverse to the fibers, to generate fracture surfaces parallel to the fiber orientation and thus expose the fiber/matrix interfaces. These specimens were coated with a layer of gold ($\sim$15 nm) by sputter-coating (K-550X, Emitech Ltd.) before SEM analysis.

Results and Discussion

Surface morphologies of the carbon fibers after different treatments are shown in Figure 1. Crenulations along the fiber axis can be seen on the surface of the oxidized carbon fibers (CAox) (Figure 1a). After the incipient wetness technique, iron particles with diameters of between 20 and 55 nm were uniformly coated onto the fiber surface (Figure 1b). These particles acted as the catalyst for CNT growth, giving rise to a homogeneous layer of grafted CNTs, a few hundred nanometers in length (Figure 1c). The diameter of the CNTs grown on the surface was in the range of 21−53 nm, is consistent with the diameter of iron particles; the diameter of CNTs synthesized via CVD is considered to depend strongly on the size of the catalyst nanoparticles employed for their growth.[25] The initial oxidation of the carbon fibers before catalyst deposition was crucial. Untreated carbon fibers (CA) showed heterogeneous grafting of CNTs due to poor catalyst distribution (Supporting Information, Figure S1). Presumably, the oxygen-containing groups present after acid treatment, particularly carboxylate groups,[7,26] encouraged wetting and helped to stabilize small iron particles on the surface.

The calculated contact angles in different test liquids are reported in Table 1. It was apparent that the advancing contact angle, θ_a, in water, substantially increased after introducing CNTs onto the fiber surface; CNT-grafted surfaces indeed have been developed for their superhydrophobic effects.[27] However, θ_a decreased slightly after the thermal oxidation, as intended, due to the introduction of polar groups onto the surface of the CNTs. The receding contact angle θ_r showed a similar trend. The difference of these two contact angle values, the contact angle hysteresis,[28] dramatically increased following the CNT grafting. This change can be attributed to the increase in chemical surface

(20) Hampe, A.; Kalinka, G.; Meretz, S.; Schulz, E. *Composites* **1995**, *26*, 40–46.
(21) Meretz, S.; Linke, T.; Schulz, E.; Hampe, A.; Hentschel, M. *J. Mater. Sci. Lett.* **1992**, *11*, 1471–1472.
(22) Meretz, S.; Auersch, W.; Marotzke, C.; Schulz, E.; Hampe, A. *Compos. Sci. Technol.* **1993**, *48*, 285–290.
(23) Miller, B.; Muri, P.; Rebenfeld, L. *Compos. Sci. Technol.* **1987**, *28*, 17–32.
(24) Kalinka, G.; Leistner, A.; Hampe, A. *Compos. Sci. Technol.* **1997**, *57*, 845–851.
(25) Sinnott, S. B.; Andrews, R.; Qian, D.; Rao, A. M.; Mao, Z.; Dickey, E. C.; Derbyshire, F. *Chem. Phys. Lett.* **1999**, *315*, 25–30.
(26) Verdejo, R.; Lamoriniere, S.; Cottam, B.; Bismarck, A.; Shaffer, M. *Chem. Commun.* **2007**, 513–515.
(27) Li, S. H.; Li, H. J.; Wang, X. B.; Song, Y. L.; Liu, Y. Q.; Jiang, L.; Zhu, D. B. *J. Phys. Chem. B* **2002**, *106*, 9274–9276.
(28) Extrand, C. W.; Kumagai, Y. *J. Colloid Interface Sci.* **1997**, *191*, 378–383.

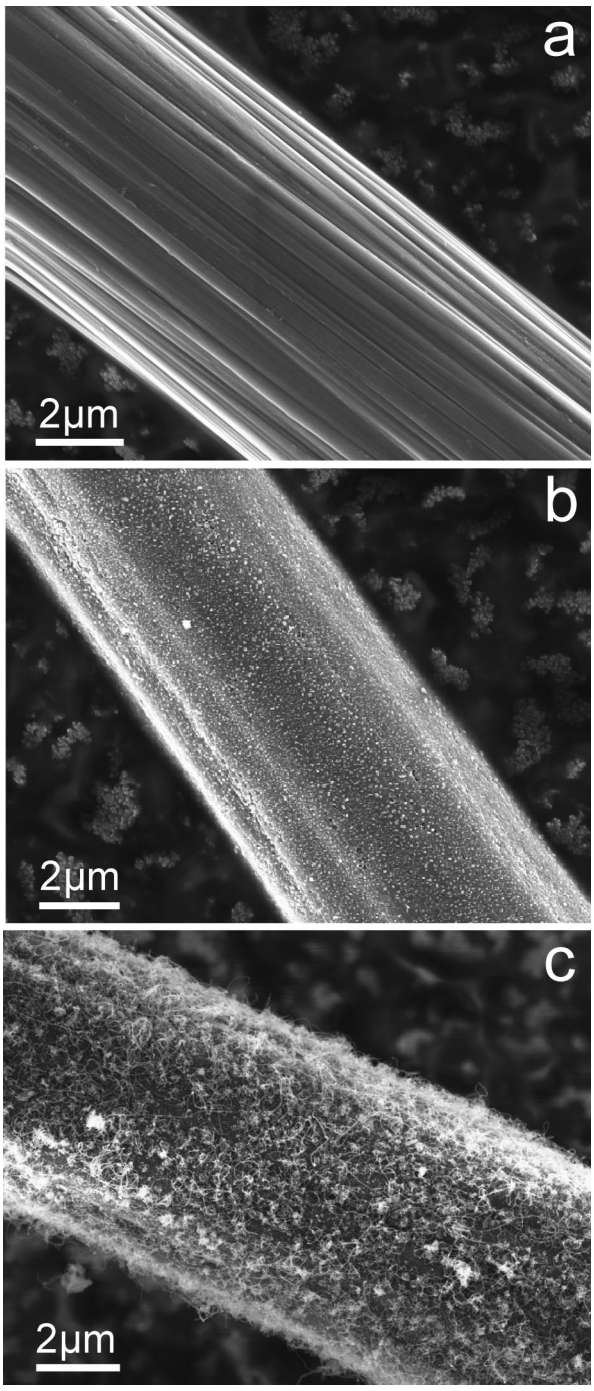

Figure 1. SEM images of carbon fibers after (a) surface oxidation, (b) deposition of iron catalyst particles, and (c) CVD growth of carbon nanotubes.

heterogeneity and surface roughness. Compared with the considerable change of contact angles in water, the contact angles of the modified carbon fibers measured in DIM showed no significant variation or hysteresis. This behavior can be attributed to the similarity of the dispersive (rather than polar) interactions for the carbon fiber and CNT surfaces, given that the values are already normalized to the (changing) surface area. The wettability of CNT-grafted carbon fibers in epoxy matrix was tested to provide a direct measure of the interaction, W_a, between the fibers and the matrix (refer to eq 4). This evaluation is only valid for the epoxy component of the matrix before the curing process but does provide a preliminary assessment of the ease of subsequent composite manufacture. The advancing contact angle measured in epoxy increased slightly after CNT grafting but after the effect was again mitigated by the thermal oxidation process, which increased the relative wettability of the CNTs. The receding contact angle was not detectable due to a relatively strong drag force induced by the high viscosity of the epoxy matrix during the emersion process.

The surface tensions of the fibers were calculated from the advancing contact angles measured in a pair of polar (water) and nonpolar (DIM) test liquids using Wu's harmonic mean equation.[18] As can be seen in Table 2, the surface tension, γ_s, and its polar contribution, γ_s^p, decreased considerably after grafting the oxidized carbon fibers with CNTs, which are relatively hydrophobic. Although the surface tension remained more or less constant after the thermal oxidation of the CNT-grafted fibers, the polar contribution substantially increased. This effect can be related to the increasing concentration of polar surface oxides,[19] giving rise to an improvement of the wettability by both water and the epoxy resin. It is generally accepted that γ_s^d reflects the essential surface characteristics of the carbon or partly graphitized carbon framework of the fiber.[17] An increase of γ_s^d was observed by introducing highly graphitized CNTs onto the fiber surface, and the value decreased after the thermal oxidation, potentially indicating a disruption of the graphitic structure of the CNTs. Thus, the CNT grafting has only a slight effect on the wettability of carbon fibers in nonpolar liquids. In addition, the thermal oxidation leads to an improved interaction with polar liquids, as indicated by the increasing surface polarity, which is likely to be advantageous for composite manufacture.

The influence of the CNT grafting on the interfacial properties of the composites was investigated by single fiber pull-out and push-out tests. The results of single fiber pull-out tests are shown in Figure 2 and Table 3. By plotting the peak force required to debond the interfacial adhesion as a function of the embedded area (Figure 2a), the apparent interfacial shear strength, τ_{app}, can be deduced from the gradient of the linear fit. The absolute values obtained can be difficult to interpret, but the technique works well as a comparative tool; values for the interfacial shear strength are frequently found to be higher than the bulk shear strength of the matrix.[29] In the current study, a significant increase of τ_{app} was observed in the composites with CNT-grafted carbon fibers. The strength increased from about 75 to 118 MPa, representing around a 60% improvement. The improvement of the interfacial performance is probably due to the increased surface area, roughness, and interfacial bonding between the CNTs and the matrix, which is consistent with the previous data shown in the literature.[3,11] Although it was difficult to obtain data across an identical range of embedded lengths, due to the delicacy of the test and the difference in strength of the fibers (see below), Figure 2b clearly shows that τ_{app} is independent of the embedded fiber length for both grafted and control fibers. This behavior has been observed

(29) Gao, S. L.; Mäder, E.; Zhandarov, S. F. *Carbon* **2004**, *42*, 515–529.

Table 1. Advancing (θ_a) and Receding (θ_r) Contact Angles in Water, Diiodomethane (DIM), and Epoxy of the Investigated Carbon Fibers Measured Using the Modified Wilhelmy Technique[a]

fiber/matrix	d (μm)	$\theta_a(H_2O)$ (deg)	$\theta_r(H_2O)$ (deg)	θ_a(DIM) (deg)	θ_r(DIM) (deg)	θ_a(epoxy) (deg)
CAox	7.2 (0.1)	47.7 (1.6)	36.2 (2.7)	46.8 (0.9)	42.8 (1.4)	58.5 (2.8)
NT-CAox	7.5 (0.2)	100.3 (1.0)	56.3 (2.6)	47.8 (1.5)	44.8 (1.3)	65.1 (2.1)
Oxi NT-CAox	7.5 (0.2)	92.2 (2.9)	44.7 (0.7)	45.0 (0.8)	43.4 (0.5)	60.3 (1.5)

[a] The standard errors are shown in the parentheses. CAox: HNO_3 oxidized carbon fibers; NT-CAox: CNT-grafted carbon fibers; Oxi NT-CAox: thermo-oxidized CNT-grafted carbon fibers.

Table 2. Solid Surface Tensions (γ_s) and Their Polar (γ_s^p) and Dispersive (γ_s^d) Components as Well as the Surface Polarity (X^p) of the Carbon Fibers and Epoxy Matrix Calculated from the Measured Advancing Contact Angle in Water and DIM[a]

fiber	γ_s (mN/m)	γ_s^p (mN/m)	γ_s^d (mN/m)	X^p
CAox	54.6 (1.4)	29.7 (1.0)	24.9 (0.4)	0.54
NT-CAox	38.8 (2.4)	1.0 (0.6)	37.8 (1.9)	0.03
Oxi NT-CAox	37.8 (3.0)	4.6 (1.4)	33.2 (1.6)	0.12

[a] The standard errors are shown in the parentheses. CAox: HNO_3 oxidized carbon fibers; NT-CAox: CNT-grafted carbon fibers; Oxi NT-CAox: thermo-oxidized CNT-grafted carbon fibers.

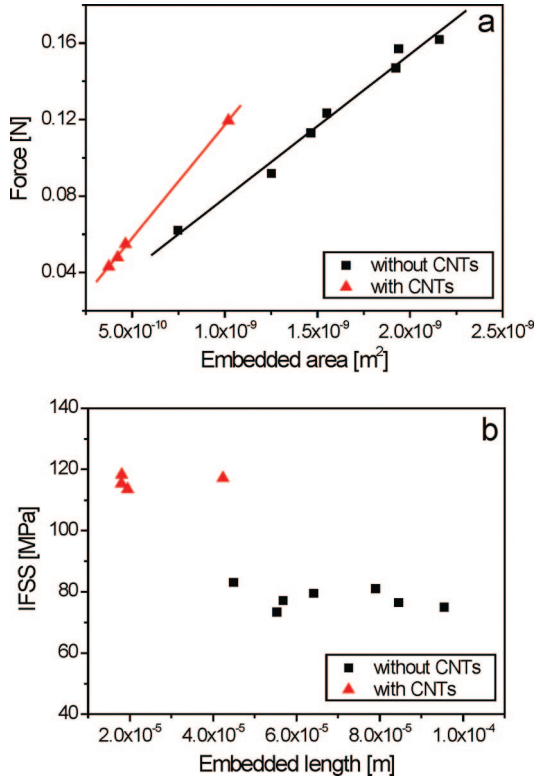

Figure 2. Single fiber pull-out test results of carbon fibers without and with CNTs on the surface. (a) Peak force as a function of embedded area. The average apparent interfacial shear strength (IFSS) is given by the gradient of linear fits. (b) IFSS as a function of embedded length. The independence of the IFSS values from the embedded length indicates a ductile type failure.

Table 3. Single Fiber Pull-Out and Push-Out Test Results for the Investigated Carbon Fibers[a]

fiber	pull-out τ_{app} (MPa)	push-out τ_{app} (MPa)
without CNTs	75.2 (4.2)	49.5 (1.4)
with CNTs	118.3 (1.9)	50.6 (2.8)

[a] The standard errors are shown in the parentheses.

previously in carbon fiber/epoxy systems[9] and indicates that the fiber/matrix interface displacement is associated with a predominantly ductile type failure.[22,30]

After the push-out tests, the composite specimens were examined by SEM, showing that the fibers had been pushed out from the matrix (Supporting Information, Figure S2). The calculated τ_{app} from the push-out tests are summarized in Table 3. Unlike the pull-out data, CNT-grafted carbon fibers exhibited no significant improvement in interfacial shear strength during the push-out tests. A hypothesis proposed to explain this difference is illustrated in Figure 3. For conventional fiber/epoxy composites, the fracture always occurs at the interface between the fiber and the matrix in both test modes.[8,24] However, CNT grafting changes the fracture mode during testing depending on the loading mechanism. In single fiber pull-out tests, the fiber is loaded from the outside, over a large region, and gradually transfers stress into the matrix, through the wetting cone, leading to fracture through the relatively strong CNT-reinforced region. On the other hand, in push-out tests, the fiber is loaded abruptly at the center, leading to internal, longitudinal, cohesive failure. The inner part of the fiber is pushed out while the outer layer remains bonded to the matrix through the CNT layer.

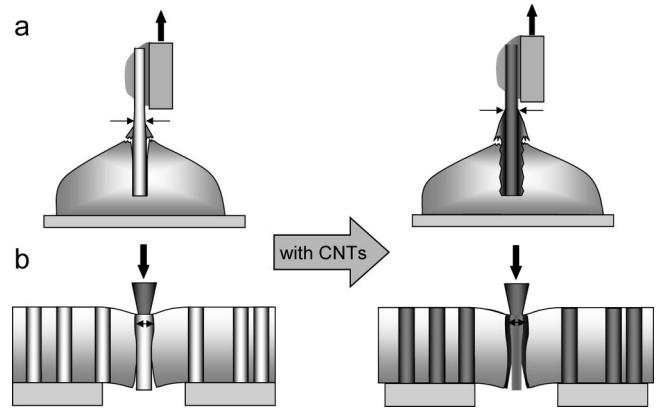

Figure 3. Schematic diagrams of the proposed failure mechanisms for (a) single fiber pull-out and (b) push-out before and after growing carbon nanotubes onto the fiber surface.

This mechanistic interpretation is supported by the fractographic analysis of composite specimens; typical SEM images of the fibers and imprints taken from the fracture surfaces are displayed in Figure 4a−e. For the composites without CNTs, the fracture morphology was consistent with transverse (intralaminar) fracture, with the fracture plane at the fiber/matrix interface and the fiber crenulations clearly visible (Figure 4a).[31] The fracture surface of the composites with CNT-grafted fibers (Figures 4c−e) presented completely different morphologies, with the fibers exhibiting an unusual rough surface. It was apparent that the failure plane was within the fibers rather than at the interface (Figure 4e). The outer layers of the fibers were peeled off during the fracture process, with the fiber diameter reduced from around 7.5 to

(30) Ramanathan, T.; Bismarck, A.; Schulz, E.; Subramanian, K. *Compos. Sci. Technol.* **2001**, *61*, 1703–1710.

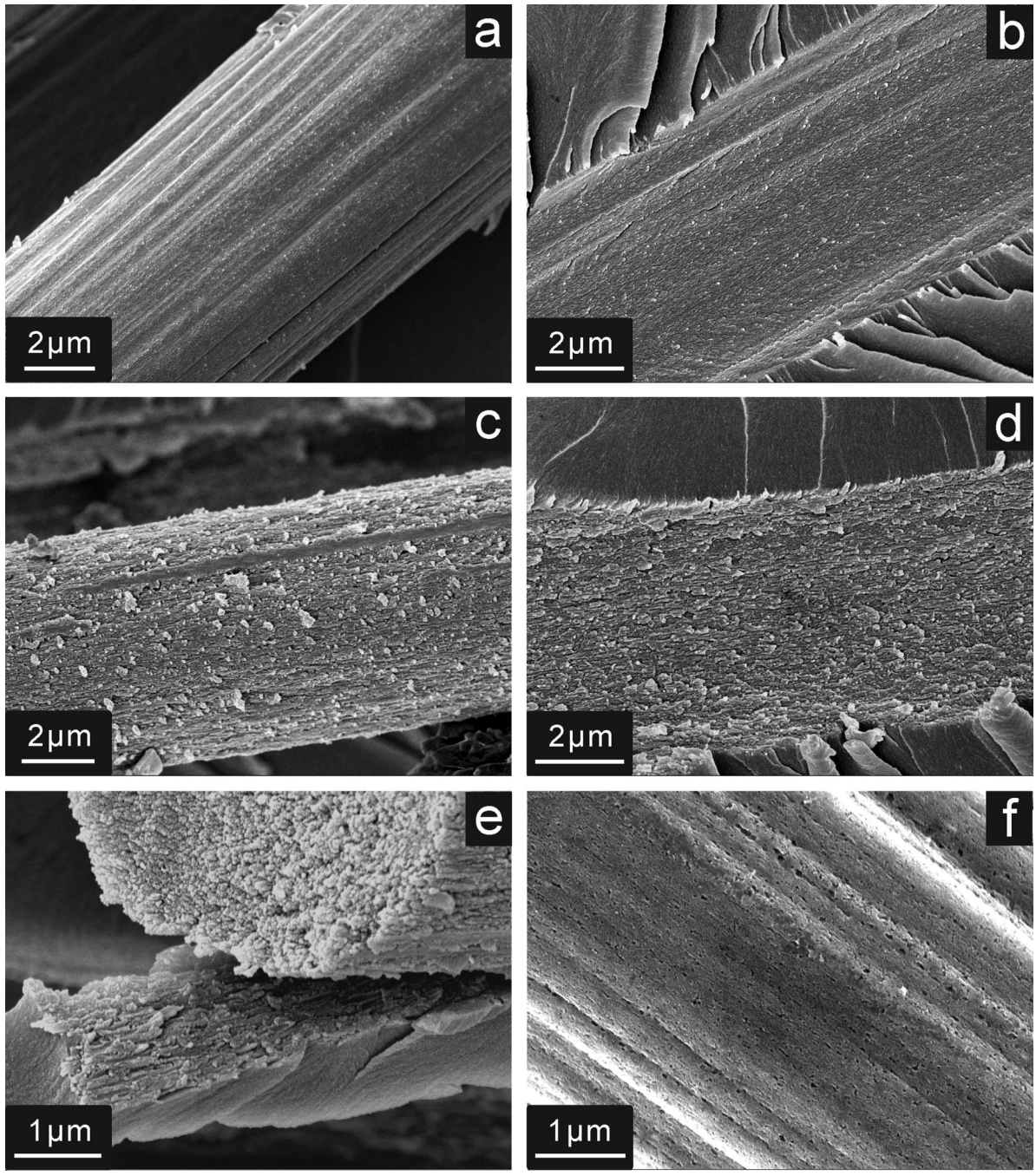

Figure 4. SEM images of the fracture surfaces of (a, b) carbon fibers/epoxy composites and (c−e) CNT-grafted carbon fibers/epoxy composites. (f) An SEM image of a catalyst loaded carbon fiber after the HCl etching.

6.7 μm. This fractographic study supports the cohesive failure hypothesis discussed above. In addition, small holes were observed on some fracture surfaces of the CNT-grafted fiber composites. To explore the formation of these holes, iron predeposited carbon fibers (Figure 1b) were washed with a hydrochloric acid (0.36 M HCl, Fluka). This etching process removed the iron to reveal numerous pits with diameters in a range of 19–61 nm, uniformly distributed on the fiber surface (Figure 4f). Such pits were not observed on HCl-treated carbon fibers without deposition of iron nanoparticles (Supporting Information, Figure S3a). The formation of the pits can be attributed to the dissolution of iron into the carbon fibers at the reaction temperature and its subsequent removal by the HCl etching process. These features are likely to weaken the outer layers of the fibers, leading to the type of unusual cohesive failure observed.

To explore the effects of this surface damage on the properties of the carbon fibers, single-fiber tensile tests were carried out at three different gauge lengths; the results are given in Table 4. The tensile strength, σ_f, and modulus, E_f, are plotted versus the gauge length in Figure 5. The modified carbon fibers lost nearly 55% of their original strength after the CNT grafting process. The degradation can be attributed to the surface damage of the fibers discussed above, i.e., the iron etching shown in Figure 4f. However, the tensile

(31) Greenhalgh, E.; Hiley, M. *Failure Analysis and Fractography of Polymer Composites*; Woodhead Publishing, in press.

Table 4. Single Fiber Tensile Test Results for the Investigated Carbon Fibers Determined at Different Gauge Lengths[a]

fiber	gauge length (mm)	tensile strength (MPa)	tensile modulus (GPa)
without CNTs	15	3990 (170)	245 (2)
	25	3500 (170)	247 (1)
	35	3320 (130)	245 (1)
with CNTs	15	1840 (100)	246 (4)
	25	1590 (110)	240 (2)
	35	1450 (70)	246 (2)

[a] The standard errors are shown in the parentheses.

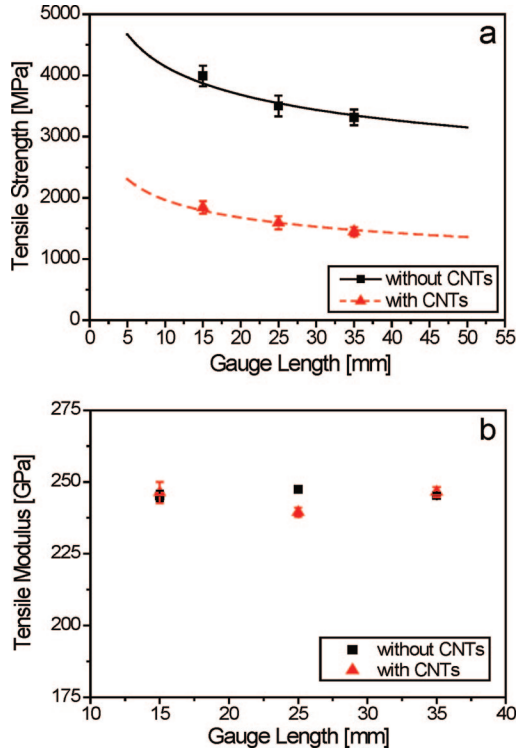

Figure 5. (a) Tensile strength and (b) tensile modulus plotted as a function of gauge length for the investigated carbon fibers. The Weibull distribution (shown as lines) in (a) accounts for the gauge length dependency of the tensile strength.

modulus of the fibers was unaffected (Figure 5b), suggesting an undamaged fiber core. It is well-known that the flaw-induced nature of fiber failure results in a length dependence for its tensile strength.[32] Indeed, the average tensile strength of all the fibers decreased as the gauge length increased. The Weibull distribution[33] was calculated to account for the length dependency, and the fitted curves are shown in Figure 5a. This good correlation between the Weibull predictions and the experimental data with increasing gauge length indicated that the surface damage is relatively homogeneous and consistent with a uniform distribution of nanoscale pits over the whole fiber surface.

In an attempt to reduce the fiber surface damage by preventing the dissolution of iron into carbon, reaction temperatures below 723 °C (the eutectic temperature in the iron−carbon phase diagram) were used for the catalyst reduction and the CVD growth processes. As a result, the loss of the tensile strength was reduced to 35%. In fact, iron-loaded fibers exhibited no pitting when heated to 700 °C. Only the carbon fibers taken to a reaction temperature above 720 °C displayed pits, presumably due to increased solubility of carbon in iron above the eutectic temperature of 723 °C (Supporting Information, Figure S3b,c). However, CNT growth below the eutectic temperature was not successful, possibly due to the same low solubility of carbon in the iron catalyst. Although surface diffusion driven growth is known,[34] crystallinity is usually lower and reaction conditions different than the more common bulk diffusion mechanism.[35] The study of alternative methods to reduce the surface damage caused by the CNT grafting is currently underway.

Conclusions

CNT-grafted carbon fibers have been successfully produced using the incipient wetness technique to load catalyst for subsequent CVD synthesis. Contact angle measurements revealed a polarity change of the fiber surface before and after the growth reaction; the reduced wettability of the rough, hydrophobic, CNT surface can be mitigated to some extent by simple thermal oxidation. The interfacial shear strength of the composites with grafted CNTs exhibited around a 60% improvement in single fiber pull-out tests but remained unchanged in the push-out geometry. This discrepancy was provisionally attributed to a change of failure mechanism between the two types of tests. Specifically, the catalyst particles damage the outer layers of the carbon fibers during the CNT growth process, leading to cohesive failure in push-out tests and a reduced tensile strength. Nevertheless, a basic strategy for improving interfacial performance of fiber composites has been demonstrated, using a simple method to attach CNTs to carbon fibers, forming a hierarchical reinforcing structure. The approach has wider implications than simply increasing IFSS; it provides a controlled means of introducing high loadings of oriented nanotubes into the matrix of conventional fibers composites. In principle, with development, the methodology should yield undamaged carbon fibers grafted with an ideal radial arrangement of CNTs, perpendicular to the primary fibers. As noted in the Introduction, the CNTs will then reinforce the matrix and have the potential to address some of the critical weaknesses of conventional fiber composites. Having recognized the potential of the approach, there are a large number of system parameters that merit exploration, including nanotube grafting density, length, diameter, crystallinity, "waviness", and surface chemistry. All these factors can be adjusted, in principle, during the CVD synthesis process; different optimal geometries are likely to emerge for particular composite systems and critical properties.

Acknowledgment. The authors thank DSTL and QinetiQ for the financial and technical support of this work and Hexcel for supplying the resin. The authors also thank Kingsley KC Ho, Steven Lamorinière (PaCE, Imperial College London), and Martina Bistritz (BAM, Berlin) for their assistance on the single

(32) Park, S. J.; Seo, M. K.; Kim, H. Y.; Lee, D. R. *Colloid Interface Sci.* **2003**, *261*, 393–398.
(33) Stoner, E. G.; Edie, D. D.; Durham, S. D. *J. Mater. Sci.* **1994**, *29*, 6561–6574.
(34) Hofmann, S.; Csányi, G.; Ferrari, A. C.; Payne, M. C.; Robertson, J. *Phys. Rev. Lett.* **2005**, *95*, 036101.
(35) Baker, R. T. K. *Carbon* **1989**, *27*, 315–323.

fiber pull-out and the push-out testing and Dr. Robin Olsson (The Composites Centre, Imperial College London) for valuable discussions.

Supporting Information Available: SEM images of raw carbon fibers before and after the growth of carbon nanotubes (Figure S1), composite specimens after the push-out test (Figure S2), and different carbon fibers after the HCl etching (Figure S3). This material is available free of charge via the Internet at http://pubs.acs.org.

CM702782J